

CO₂ gas resonance absorption at CO₂ laser wavelength in multiple laser coating

L. Jiang · L. Li · H.-L. Tsai

Received: 7 January 2009 / Revised version: 25 March 2009 / Published online: 2 May 2009
© Springer-Verlag 2009

Abstract Multiple laser beams demonstrate many advantages as energy sources in diamond synthesis. In a reported amazingly-fast multiple laser coating technique, CO₂ gas is claimed as the sole precursor or secondary precursor for forming a diamond or diamond-like carbon, which remains poorly understood. The absorption coefficient changes under the irradiation of multiple lasers are one of the keys to resolve the mysteries of multiple laser beam coating processes. This study investigates the optical absorption in CO₂ gas at the CO₂ laser wavelength. The resonance absorption process is modeled as an inverse process of the lasing transitions of CO₂ lasers. The well-established CO₂ vibrational-rotational energy structures are used as the basis for the calculations with the Boltzmann distribution for equilibrium states and the three-temperature model for non-equilibrium states. Based on the population distribution, our predictions of the CO₂ absorption coefficient changes as a function of temperature are in agreement with the published data.

PACS 78.20.Bh · 42.62.Cf · 76.20.+q

L. Jiang (✉)
Laser Micro-/Nano-Fabrication Laboratory, School of Mechanical Engineering, Beijing Institute of Technology, 100081 Beijing, People's Republic of China
e-mail: jianglan@bit.edu.cn

L. Li
School of International Co-Education, Beijing Institute of Technology, 100081 Beijing, People's Republic of China

H.-L. Tsai
Laser-Based Manufacturing Laboratory, Department of Mechanical and Aerospace Engineering, Missouri University of Science and Technology (Formerly University of Missouri-Rolla), Rolla, MO 65409, USA

Nomenclature

a :	average interatomic spacing
A_{21} :	spontaneous transition probability (rate)
E_j :	energy level
g_{001} :	rotational statistical weights of quantum levels of 001
g_{100} :	rotational statistical weights of vibrational quantum levels of 100
h :	Planck constant
j :	index in the numerator in (6)
j' :	index in the denominator in (6)
k_B :	Boltzmann constant
K :	constant in (4)
l :	length of the laser-gas interaction zone
n :	constant in (4)
n_0 :	populations of the ground state
n_1 :	populations of the 100 state
n_2 :	populations of the 010 state
n_3 :	populations of the 001 state
n_{abs} :	number density of the gas
N :	total number of molecules
$N_{p,\text{abs}}$:	average number of absorbed photons
$P(\Psi)$:	population densities
P_g :	gas pressure
$R\Pi$:	twofold vibrational degeneracy of Π states
T :	temperature
T_1 :	vibrational temperature of 100
T_2 :	vibrational temperature of 010
T_3 :	vibrational temperature of 001
T_{tr} :	translational temperature
T_{rot} :	rotational temperature
T_c :	characteristic temperature
Z :	partition function

Greek symbols

α :	absorption coefficient
λ :	wavelength
τ :	radiative life time for the transition
σ :	absorption cross section
ν_0 :	frequency at the line center
ν_c :	optical broadening collision frequency
$\Delta\nu_0$:	full width at half-maximum
ν_1 :	base frequencies of the harmonic oscillators of symmetric stretch mode
ν_2 :	base frequencies of the harmonic oscillators of bending mode
ν_3 :	base frequencies of the harmonic oscillators of asymmetric stretch mode

1 Introduction

Laser-assisted diamond synthesis processes, especially multiple laser beam coating techniques, demonstrate unique advantages over conventional methods [1–7]. However, the fundamental mechanisms involved in the processes are not well understood [1, 5–10]. In a reported high-speed multiple laser coating process [5–7], CO₂ gas is claimed as the sole precursor or secondary precursor for forming a diamond or diamond-like carbon, which remains poorly understood and unverified. This astonishing coating technique [5–7] needs further careful scientific investigation and substantiation.

The absorption coefficient changes under the irradiation of the multiple lasers are one of the keys to resolve the mysteries of multiple laser beam coating processes. As a first theoretical step, this study investigates the optical absorption in CO₂ gas at the CO₂ laser wavelength. Strilchuk and Offenberger [11] measured the resonant absorption coefficient in CO₂ gas at 350–1600 K. Their results were compared with the theory of Munjee and Christiansen [12] for mixed mode contributions to absorption. The experiment was an extension of the earlier simple measurements of absorption in CO₂ at 10.6 μm wavelength by Gerry and Leonard [13]. However, the CO₂ gas being irradiated by a laser can be in a non-equilibrium state, in which energy distributions at different levels cannot be characterized by a single temperature. Vibrational, translational and rotational energies shall be characterized by their own temperatures individually. Hence, a five-temperature model and a three-temperature model were introduced for laser heating of CO₂ gas [14, 15].

This paper investigates the resonance absorption process as an inverse process of the lasing transitions of CO₂ lasers. The calculated temperature-dependent absorption coefficient will then be incorporated in a 3D CO₂ gas flow model to consider the fluid properties such as species, pressures, velocities, and temperatures in coating processes. This will

further be used to theoretically reveal the role of the CO₂ laser in multiple laser coating.

In this study, the well-established CO₂ vibrational-rotational energy structures [14] are used as the basis for the calculations: each vibrational energy level is modeled as a quantum harmonic oscillator with a characteristic frequency and the thermal distribution of rotational levels. In equilibrium states, the populations at excited vibrational-rotational energy states are determined by the Boltzmann distribution at a certain translational temperature. In the non-equilibrium states induced by powerful laser irradiation, the three-temperature model (translational temperature and vibrational temperatures for the excited levels of 001 and 100) [15, 16] is used to calculate the excited-state populations.

2 Modeling

2.1 Absorption coefficient

The absorption coefficient changes under the irradiation of multiple lasers are one of the keys to resolve the mysteries of multiple laser beam coating processes. The resonance absorption of CO₂ lasers by CO₂ gas is basically an inverse process of the lasing transitions of CO₂ lasers.

Considering the transition from 100 to 001, the resonance absorption coefficient at the wavelength of 10.6 μm can be written as [11–13]

$$\alpha(\lambda) = \frac{1}{4\pi} \frac{\lambda^2}{\tau} \left(\frac{g_{001}}{g_{100}} n_{100} - n_{001} \right) \frac{1}{\nu_c}, \quad (1)$$

where g_{001} and g_{100} are the rotational statistical weights for rotational-vibrational quantum levels of 001, 100; α is the absorption coefficient; λ is the wavelength; ν_c is the optical broadening collision frequency; and τ is the radiative life time for the transition. For each contributing transition where the line is collision-broadened, (1) can be applied. For instance, at the wavelength of 9.6 μm, the corresponding quantum levels are 001 and 020/010.

The radiative life time for the transition, τ , is given by [11, 12]

$$\frac{2}{\tau} = A_{21} = \left(\frac{64\pi^3}{3h} \right) \left(\frac{1}{\lambda^3} \right) \left\{ \frac{S(J_2)K_{21}}{g_{001}} \right\}, \quad (2)$$

where A_{21} is the spontaneous transition probability (rate) and h is the Planck constant. In (2), for a P-branch transition, $S(J_2) = J_2 + 1$ and for a R-branch transition, $S(J_2) = J_2$ (where J_2 is the rotational number of 010 state whose value depends on the transition process [11]). K_{21} is the J independent part of the square of the matrix element of the dipole moment. The rotational-vibrational constants of different bands are given in reference [12]. A collision Lorentzian

profile is assumed for the line shape of a single transition at the given wavelength in (1):

$$\frac{1}{v_c} = \frac{(\Delta\nu_c/2\pi)}{1/[(\nu - \nu_0)^2 + (\Delta\nu_c/2)^2]}, \quad (3)$$

where ν_0 is the frequency at the line center; $\Delta\nu_c$ is the full width at half-maximum, which may be written

$$\Delta\nu_c = \frac{2C_{\text{CO}_2} P}{(8\pi k_B T)^{1/2}}, \quad C_{\text{CO}_2} = K T^n, \quad (4)$$

where K and n are constants. K can be determined by the data from previous measurements [11, 17]: $\Delta\nu_c = 5.97 \times 10^9$ Hz at pressure: $P_g = 1$ atm and temperature: $T = 300$ K.

For different transitions due to the near resonant absorption from mixed modes, the total absorption coefficient is obtained by repeatedly applying (1)–(4) to the contributing transitions and summing:

$$\alpha(\lambda) = \alpha_{P\Sigma}(\lambda) + \alpha_{R\Sigma}(\lambda) + \alpha_{2R\Pi}(\lambda), \quad (5)$$

where $R\Pi$ is the twofold vibrational degeneracy of the Π states and the Π states are treated as though they were vibrationally nondegenerate.

At a fixed wavelength, the absorption coefficient is a function of the populations of both the lower and upper levels of the rotational-vibrational transition (for example, at 10.6 μm, 100 and 001 state). By calculating the populations of the lower and upper levels of the rotational-vibrational transition, the absorption coefficient and its variation with temperature can be determined. Population densities are determined by the Boltzmann distribution in equilibrium states or the three-temperature model in non-equilibrium states.

2.2 Boltzmann distribution

If the CO₂ gas is in equilibrium states, all translational temperature and vibrational temperatures are equal to each other. The population densities at different energy levels can be described by the Boltzmann distribution:

$$P(\Psi_j) = \frac{\exp(-E_j/kT)}{\sum_{j'} \exp(-E_{j'}/kT)}, \quad (6)$$

where $P(\Psi_j)$ is the population densities at different energy levels; E_j is the energy level; j' in the denominator is distinct from the index j in the numerator. Use the definition of the partition function:

$$Z \equiv \sum_{j'} \exp(-E_{j'}/kT). \quad (7)$$

In equilibrium states, the Boltzmann distribution can be applied to all the vibrational states including highly excited states, for example:

100, 200, 300, 400, 500, ..., q00 (energy level: $q\hbar\nu_1$),

010, 020, 030, 040, 060, ..., 0m0 (energy level: $m\hbar\nu_2$),
001, 002, 003, 004, 005, ..., 00i (energy level: $i\hbar\nu_3$).

For the quantum harmonic oscillator ν_1 (asymmetric stretch),
 $n_{100} = n_0 \exp(-\hbar\nu_1/kT_1) = n_0 \exp(-T_{c1}/T_1)$,
 $n_{200} = n_0 \exp(-2\hbar\nu_1/kT_1)$,
 $n_{300} = n_0 \exp(-3\hbar\nu_1/kT_1)$,

where n_0 is the population of the ground state, and T_{c1} is the characteristic temperature of the quantum harmonic oscillator ν_1 .

Since $\hbar\nu_1$ is very small compared with the ionization potential and the population exponentially decreases with q ,

$$\begin{aligned} \sum_q n_{q00} &\approx \sum_{q=1}^{\infty} n_{q00} = \sum_{q=1}^{\infty} n_0 \exp(-q\hbar\nu_1/kT_1) \\ &= \frac{n_0 \exp(-\hbar\nu_1/kT_1)}{1 - \exp(-\hbar\nu_1/kT_1)}, \end{aligned}$$

where n_{q00} represents the population of the $q00$ (energy level: $q\hbar\nu_1$) state.

Then,

$$\sum_q n_{q00} \approx \frac{n_0 \exp(-T_{c1}/T_1)}{1 - \exp(-T_{c1}/T_1)}. \quad (9)$$

A similar equation can be applied for ν_2 (symmetric stretch mode) and ν_3 (bending mode). Then, the partition function can be obtained by

$$Z = n_0 + \sum_q n_{q00} + \sum_m n_{m00} + \sum_i n_{i00}. \quad (10)$$

The population probability at a specific state is given by

$$p_{qmi} = \frac{n_{qmi}}{Z}. \quad (11)$$

2.3 Three-temperature model

Under laser irradiation, the CO₂ gas can be in a non-equilibrium state, in which energy distributions at different levels cannot be characterized by a single temperature. However, within each of the vibrational modes, the levels are strongly coupled by collisions to reach equilibrium and can be represented by the same temperature [14] because the thermalization process is very fast due to a small energy difference within the same mode as compared with those of intermodes. Hence, within each mode, the Boltzmann distribution can be established much faster than the intermode distributions. Since each mode can be considered independent, it can have its own temperature. Knowing the temperatures, it is possible to determine the population density of any level.

In addition to vibrational temperatures, the translational and rotational energies can also be described by their temperatures. For CO₂, five temperatures can be defined: T_{tr} (translational temperature); T_{rot} (rotational temperature); T_1 , T_2 , and T_3 for three excited vibrational levels. However, the rotational-translational energy transport is fast, so $T_{\text{tr}} = T_{\text{rot}}$. Because of the accidental degeneracy between 100 and 020, it is reasonable to assume that $T_1 = T_2$. Thus only three independent parameters are required to describe the laser generated nonequilibrium rotational-vibrational distribution for CO₂ molecules. The populations over the vibrational levels of each of these modes are described by the Boltzmann distributions with vibrational temperatures T_i ($i = 1, 2, 3$) for CO₂:

$$\begin{aligned} n_1 &= n_0 \exp(-hv_1/kT_1), \\ n_2 &= 2n_0 \exp(-hv_2/kT_2), \\ n_3 &= n_0 \exp(-hv_3/kT_3), \end{aligned} \quad (12)$$

where n_0 , n_1 , n_2 , and n_3 are the populations of the ground state, and 100, 010, and 001 states respectively; v_1 , v_2 , and v_3 are the base frequencies of the harmonic oscillators for the excited vibrations $v_1 = 4.2 \times 10^{13}$ Hz; $v_2 = 2 \times 10^{13}$ Hz; and $v_3 = 7 \times 10^{13}$ Hz [14]. For each vibrational model, a characteristic temperature, T_c , is defined so that the product of the Boltzmann constant k_B and the characteristic temperature is equal to the vibrational energy space: $kT_{ci} = hv_i$. For CO₂, $T_{c1} = 2000$ K, $T_{c2} = 960$ K, and $T_{c3} = 3380$ K.

From the conservation of the vibrational energy,

$$e_{\text{vib}}^* = e_{\text{vib}} + \frac{N_{p,\text{abs}}}{N} k_B (T_{c3} - T_{c1}), \quad (13)$$

which can be interpreted as the energy increase by the laser excitation being equal to the total energy of the average number of photons absorbed per molecule. In (13), * means the excitation state, N is the total number of molecules and $N_{p,\text{abs}}$ is the average number of absorbed photons per molecule.

The absorbed photon energy is equal to the difference between the v_3 mode energy during and before the laser pulse,

$$\frac{N_{p,\text{abs}}}{N} k_B T_{c3} = \frac{k_B T_{c3}}{\exp(T_{c3}/T_3) - 1} - \frac{k_B T_{c3}}{\exp(T_{c3}/T) - 1}. \quad (14)$$

Thus,

$$T_3 = \frac{T_{c3}}{\ln\left(\frac{k_B T_{c3}}{\left(\frac{N_{p,\text{abs}}}{N} k_B T_{c3} + \frac{k_B T_{c3}}{\exp(T_{c3}/T)-1}\right)} + 1\right)}, \quad (15)$$

where T is the initial temperature before the excitation. The average number of absorbed photons, $N_{p,\text{abs}}$, is determined by

$$N_{p,\text{abs}} = N_{p,\text{inc}} n_{\text{abs}} \sigma l, \quad (16)$$

where n_{abs} is the number density of the laser-interacted species (gas) that is determined by the pressure; σ is the absorption cross section; l is length of the laser-gas interaction zone.

After the CO₂ laser excitation, the vibrational energies for CO₂ can be written as follows (note that v_2 is doubly degenerate):

$$\begin{aligned} e_{\text{vib}} &= \frac{k_B T_{c1}}{\exp(T_{c1}/T_1) - 1} + \frac{2k_B T_{c2}}{\exp(T_{c2}/T_2) - 1} \\ &\quad + \frac{k_B T_{c3}}{\exp(T_{c3}/T_3) - 1}. \end{aligned} \quad (17)$$

Before the CO₂ laser irradiation, the vibrational energies for CO₂ are

$$\begin{aligned} e_{\text{vib}} &= \frac{k_B T_{c1}}{\exp(T_{c1}/T) - 1} + \frac{2k_B T_{c2}}{\exp(T_{c2}/T) - 1} \\ &\quad + \frac{k_B T_{c3}}{\exp(T_{c3}/T) - 1}, \end{aligned} \quad (18)$$

where it is assumed that $T_{\text{tr}} = T_1 = T_3$ before the CO₂ laser irradiation.

Using $T_1 = T_2$, $T_3/T_{c3} = T_1/T_{c1}$, and the equations explained earlier, the excited temperature (or energy) distributions can be obtained.

In fact, the dimensionless mathematic description in this section is greatly simplified from the reality. For more realistic modeling, the three-temperature model should be combined with a 3D CO₂ gas flow model [15]. Also, the absorption coefficient changes explained earlier should be included, which is critical for multiple laser interactions in multiple laser beam coating processes.

For comparison purposes, the initial temperatures and pressures of the CO₂ gas are selected based on the published experiment conditions [11, 12]. In our calculations, the CO₂ laser operation parameters (PRC XL1500) are assumed to have

Power: 50–1500 W

CW mode

Beam diameter: 0.3–14 mm

Irradiation time: 1 second

3 Results and discussion

3.1 Population densities

Shown in Fig. 1, as expected, we see that populations of the ground state and higher excited levels are monotonous functions of the temperature. For example, at room temperature,

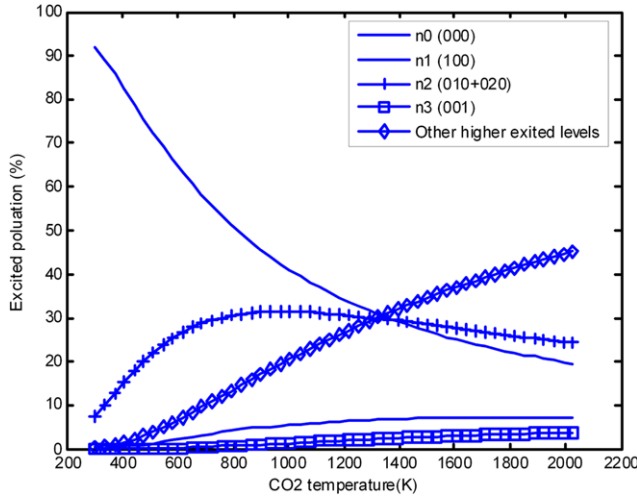


Fig. 1 Population densities in equilibrium states as functions of the temperature

most molecules are in ground states,

$n_0 (000)$	92%,
$n_1 (100)$	0.1%,
$n_2 (010 + 020)$	7.6%,
$n_3 (001)$	0.001%,
Other	0.3%,

while at 2000 K, the higher excited states become populated:

$n_0 (000)$	19.9%,
$n_1 (100)$	7.3%,
$n_2 (010 + 020)$	24.5%,
$n_3 (001)$	3.6%,
Other	44.7%.

Larger populations at higher energy levels imply that more possible contributing transitions may be involved, which tends to increase the absorption coefficient. Hence, generally speaking, a higher temperature typically leads to higher absorption coefficients, which was also experimentally observed [18, 19]. However, this tendency may not always be true, especially for resonance absorptions, in which the population densities at specific levels dominate the light-matter interaction. For CO₂ gas at the wavelength of 10.6 μm, according to (1), the populations at 001 and 100 are critical. At the wavelength of 9.6 μm, the populations at 001 and 010/020 are critical. Figure 1 shows that the population at 010 and 020 increases with the gas temperature to about 1000 K and then decreases.

For CO₂ gas at the wavelength of 10.6 μm, 001 (n_3) and 100 (n_1) are most important. Figure 2 shows the population distributions of the symmetric stretch mode with the characteristic frequency of ν_1 . At room temperature, higher excited states (200, 300, 400, ...) are almost empty. At 2000 K, the

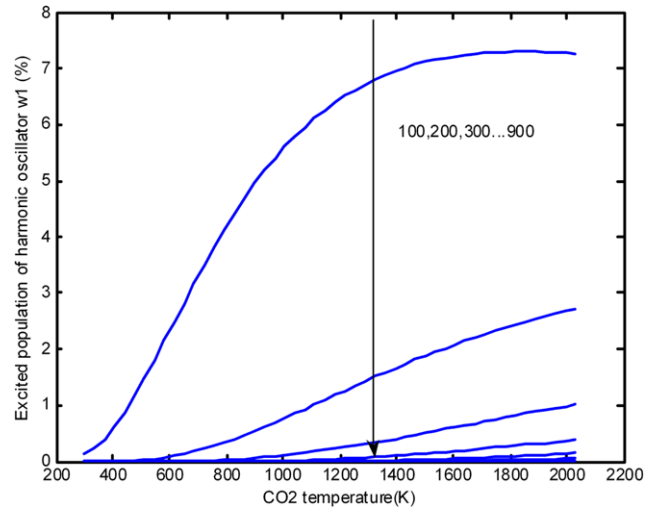


Fig. 2 Population of the quantum harmonic oscillator with the characteristic frequency of ν_1

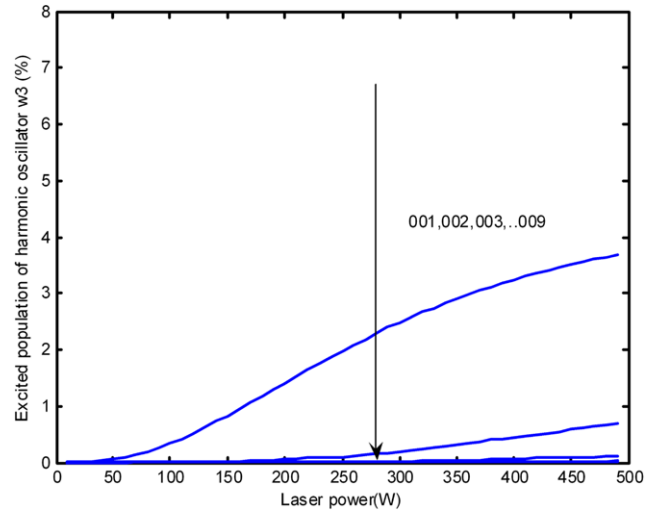
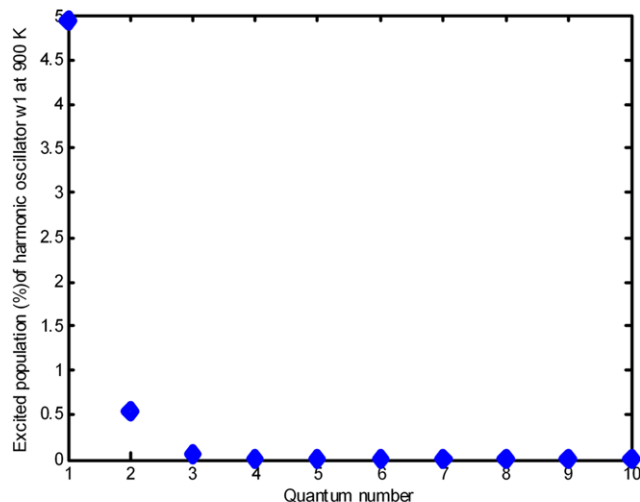
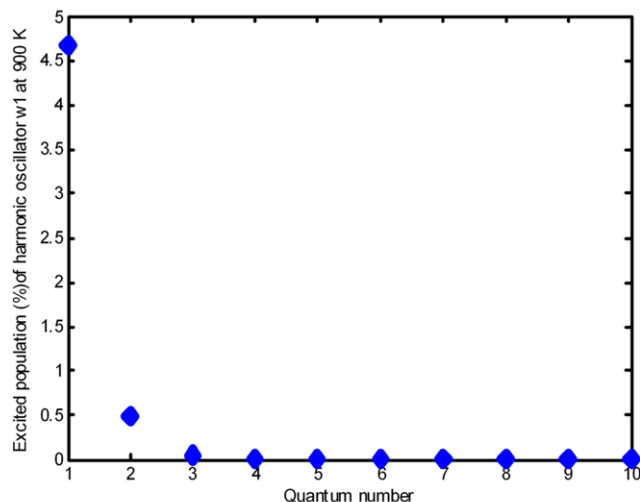


Fig. 3 Population of the quantum harmonic oscillator with the characteristic frequency of ν_3

population at the energy level of 200 is 2.7% and at the energy level of 300 is 1%. The case of asymmetric stretching is shown in Fig. 3, which demonstrates similar observations with that of the symmetric stretching. However, the populations of the asymmetric stretch mode are even lower due to the higher characteristic frequency of the harmonic quantum oscillators. In non-equilibrium states under the laser irradiation, as expected, the population of 100 (ν_1) decreases, because some molecules are excited to the state of 001 (ν_3) as shown Figs. 4 and 5. At the wavelength of 10.6 μm, the populations of 100 and 001 can become the same due to laser-induced saturation, as shown Figs. 4(b) and 5(b).

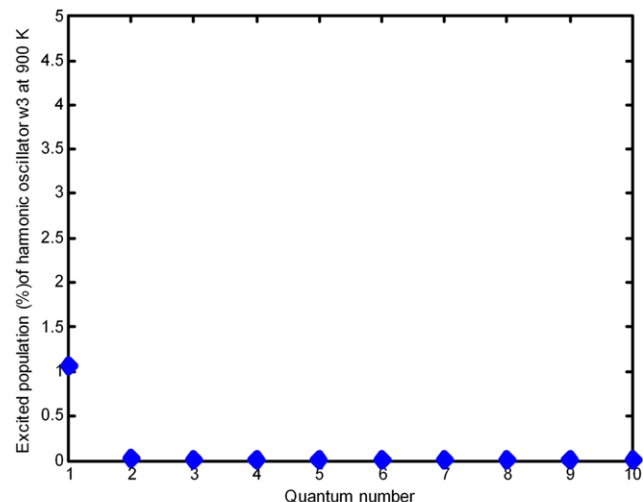
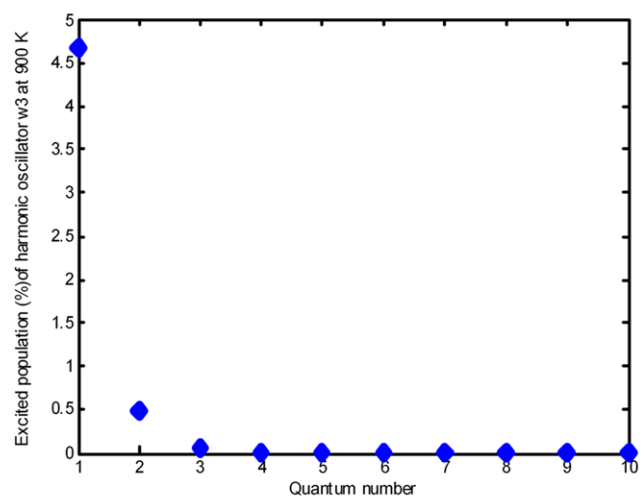
**a** Equilibrium state**b** Non-equilibrium state**Fig. 4** Population of the quantum harmonic oscillator with the characteristic frequency of ν_1 at 900 K

3.2 Absorption coefficient

According to the previous analysis, at high temperatures, the absorption calculation is complex due to the large number of transition possibilities. Hence, our model in this paper for the absorption coefficient is intended for a temperature lower than 1800 K.

According to (1), if the wavelength is fixed, for example, 10.6 μm , the resonance absorption coefficient is a function mainly of the populations of 001 and 100 states. In this case, by combining the coefficients, the equation can be explicitly written as

$$\alpha = c_{100}n_{100} - c_{001}n_{001}. \quad (19)$$

**a** Equilibrium state**b** Non-equilibrium state**Fig. 5** Population of the quantum harmonic oscillator with the characteristic frequency of ν_3 at 900 K

Similarly, for the wavelength of 9.6 μm , the corresponding absorption coefficient can be expressed as a function of 001 and 020 (010).

As shown in Fig. 6, at low temperatures (<500 K), the absorption coefficient of CO₂ gas at 10.6 μm is linearly proportional to the population of the energy level 100. But at higher temperatures, the population of 001 must be included, as shown in Figs. 6 and 7. Our predictions are in agreement with the experimental data, shown in Fig. 7, which validates the effectiveness of our model in the given temperature range. Also, the increase of absorption coefficient with temperature can play a key role in photodissociation and ionization of CO₂ gas in multiple laser beam coating.

At low temperatures, the CO₂ resonant absorption at 10.6 μm is dominated by the populations of the 001 and 100 states. Hence, (19) is a good approximation for the reso-

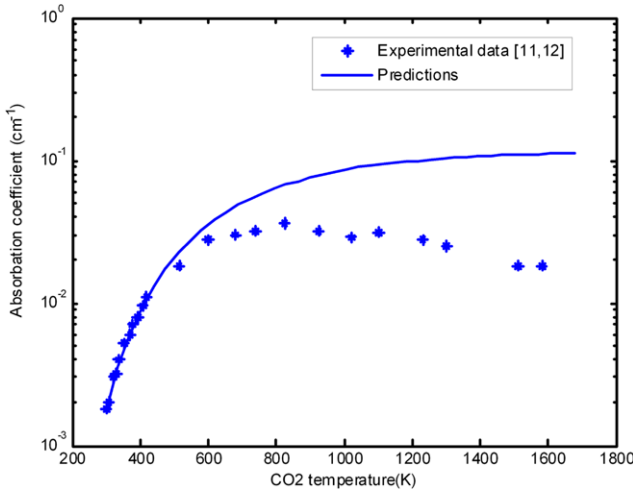


Fig. 6 Absorption coefficient calculated by the lower level of the rotational-vibrational transition only

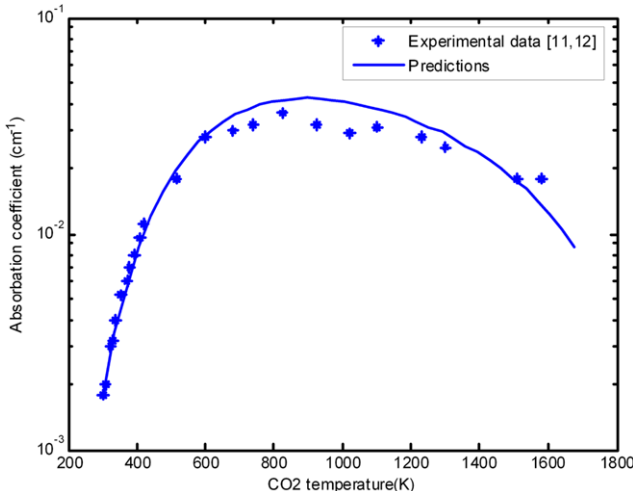


Fig. 7 Absorption coefficient calculated by the populations of both the lower and upper level of the rotational-vibrational transition

nance absorption at low temperatures as shown in Fig. 7. At higher temperatures, larger populations at higher energy levels imply that more possible contributing transitions may be involved, which makes excitations at higher energy levels play a more important role. Hence, (19) works less accurately at higher temperatures, as shown in Fig. 7. Thus, (19) is used for temperatures lower than 1800 K in this study.

4 Conclusions

This study investigates the optical absorption in CO₂ gas at the CO₂ laser wavelength. This resonance absorption process is modeled as an inverse process of the lasing transitions of CO₂ lasers. The well-established CO₂ vibrational-rotational energy structures are used as the basis for the

calculations: each vibrational energy level is modeled as a quantum harmonic oscillator with a characteristic frequency and the thermal distribution of the rotational levels is described by the Boltzmann distribution. In equilibrium states, the populations at excited vibrational-rotational energy states are determined by the Boltzmann distribution at the same temperature. In the non-equilibrium states induced by powerful laser irradiation, a three-temperature model is used to calculate the excited-state populations. Our predictions of the CO₂ absorption coefficient change as a function of temperature are in agreement with the published experimental data.

It is theoretically discovered/confirmed that (1) the population at the energy levels 010 and 020 increases with temperature to about 1000 K and then decreases, after which the higher excited states become significant; (2) at low temperatures (<500 K), the absorption coefficient of CO₂ gas at the wavelength of 10.6 μm is linearly proportional to the population at the energy level 100; and (3) at higher temperatures (500–1800 K), the absorption coefficient of CO₂ gas at the wavelength of 10.6 μm can be precisely determined by the populations at the energy levels 100 and 001. The increase of absorption coefficient with the temperature can play a key role in photodissociation and ionization of CO₂ gas in multiple laser beam coating.

Acknowledgements This work was supported by the Office of Navy Research through Multidisciplinary University Research Initiative (MURI) program USA under Grant No. N00014-05-1-0432, the 863 Project of China under Grant No. 2008AA03Z301, the National Natural Science Foundation of China under Grant No. 50705009, and the 111 project of China under Grant No. B08043.

References

1. D. Reinhard, *Diamond Thin Films Handbook* (Marcel Dekker, New York, 2001)
2. A.A. Voevodin, M.S. Donley, J.S. Zabinski, Surf. Coat. Technol. **92**(1), 42 (1997)
3. A.A. Voevodin, M.S. Donley, Surf. Coat. Technol. **82**(3), 199 (1996)
4. R. Roy, S. Gedevanishvili, E. Breval, P. Mistry, M. Turchan, Mater. Lett. **46**(1), 30 (2000)
5. P. Misery, M. Turchan, R. Roy, S. Gedevanishvili, E. Breval, Mater. Res. Innov. **3**(1), 24 (1999)
6. P. Mistry, M.C. Turchan, G.O. Granse, T. Baurmann, Mater. Res. Innov. **1**(3), 149 (1997)
7. A. Badzian, B.L. Weiss, R. Roy, T. Badzian, W. Drawl, P. Mistry, M.C. Turchan, in *The 1997 10th International Vacuum Microelectronics Conference, IVMC'97*, Kyongju, South Korea, 17–21 August 1997, p. 546 (1997)
8. R. Roy, A. Badzian, E. Breval, T. Badzian, P. Mistry, M.C. Turchan, J. Mater. Chem. **10**(10), 2236 (2000)
9. R. Peelamedu, A. Badzian, R. Roy, R.P. Martukanitz, J. Am. Ceram. Soc. **87**(9), 1806 (2004)
10. V.I. Konov, A.M. Prokhorov, S.A. Uglov, A.P. Bolshakov, I.A. Leontiev, F. Dausinger, H. Hügel, B. Angstenberger, G. Sepold, S. Metev, Appl. Phys. A **66**, 575 (1998)

11. A.R. Strilchuk, A.A. Offenberger, *Appl. Opt.* **13**, 2643 (1974)
12. S.A. Munjee, W.H. Christiansen, *Appl. Opt.* **12**, 993 (1973)
13. E.T. Gerry, D.A. Leonard, *Appl. Phys. Lett.* **8**(9), 227 (1966)
14. W.J. Witteman, *The CO₂ Laser* (Springer, New York, 1987)
15. S. Sazhin, P. Wild, C. Leys, D. Toebaert, E. Sazhina, *J. Phys. D: Appl. Phys.* **26**, 1872 (1993)
16. V.V. Nevdakh, M. Ganjali, *J. Appl. Spectrosc.* **72**(1), 75 (2005)
17. A.D. Devir, U.P. Oppenheim, *Appl. Opt.* **8**(10), 2121 (1969)
18. D.W. Mattison, M.A. Oehlschlaeger, J.B. Jeffries, R.K. Hanson, in *41st AIAA Aerospace Sciences Meeting and Exhibit*, Reno, Nevada (2003)
19. E.A. Barbour, M. Oehlschlaeger, D.W. Mattison, D.F. Davidson, C. Schulz, J.B. Jeffries, R.K. Hanson, in *UV Absorption of CO₂ for Temperature Diagnostics*, LACEA, February 9–11, 2004, Annapolis, MA (2004)